

## Evolution of $sp^2$ bonding with deposition temperature in tetrahedral amorphous carbon studied by Raman spectroscopy

M. Chhowalla,<sup>a)</sup> A. C. Ferrari, J. Robertson, and G. A. J. Amarantunga  
*University of Cambridge, Engineering Department, Cambridge CB2 1PZ, United Kingdom*

(Received 4 October 1999; accepted for publication 20 January 2000)

Two transitions in the bonding are found in tetrahedral amorphous carbon ( $ta$ -C) films as a function of deposition temperature. The total  $sp^3$  fraction shows a sharp decrease at a transition temperature of order 250 °C. In contrast, visible Raman finds that the  $sp^2$  sites show a gradual ordering into the graphitic clusters through the sharp bonding transition. The optical gap and resistivity show a similar, gradual transition. This indicates that the  $sp^2$  cluster size determines the optical gap, even when the  $sp^2$  content does not change. The Raman  $I(D)/I(G)$  peak ratio is found to vary inversely with the square of the gap. © 2000 American Institute of Physics. [S0003-6951(00)02311-1]

Tetrahedral amorphous carbon ( $ta$ -C) is characterized by high percentage (85%) of “diamond-like”  $sp^3$  bonding.<sup>1-4</sup>  $ta$ -C films can be deposited from carbon ions with energies ranging from 30 to 600 eV. The variation of the  $sp^3$  fraction as a function of the ion energy and substrate temperature has been studied and can be described by the subplantation model.<sup>3-5</sup>  $ta$ -C also contains a small fraction of  $sp^2$  bonding. It has been shown that the  $sp^3$  fraction controls the mechanical properties of  $ta$ -C, while  $sp^2$  sites primarily control the optical and electrical properties.<sup>6,7</sup>

We previously studied the variation of the  $sp^3$  fraction, optical, and electronic properties of  $ta$ -C films as a function of deposition temperature.<sup>8</sup> The  $sp^3$  fraction remains constant up to a transition temperature of about 250 °C, above which it decreases sharply to near zero. This transition has also been seen by other groups.<sup>4,9</sup> In contrast, the optical gap, refractive index, and conductivity decrease gradually from above room temperature without an abrupt transition. Similarly, it was recently found that the optical gap of  $ta$ -C deposited at room temperature decreases strongly at an annealing temperature of about 700 °C, while the  $sp^3$  fraction is stable up to 1000–1100 °C.<sup>10</sup> These results suggest that the total  $sp^3$  fraction and optical gap are not directly linked. On the other hand, the optical gap of a wide range of as-deposited amorphous carbons correlates well with their total  $sp^2$  content.<sup>11</sup> Thus the precise relationship between band gap and  $sp^2$  bonding is not clear.

This letter shows how the band gap and resistivity can vary even when the number of  $sp^2$  sites is essentially fixed. To do this, we report further on the influence of deposition temperature on the rearrangement of the  $sp^2$  sites well before the relaxation of the  $sp^3$  phase. We use Raman spectroscopy to explore the evolution of the  $sp^2$  bonding and explain how the gap and total  $sp^2$  content can vary independently.

The 50-nm-thick  $ta$ -C films were deposited using a filtered cathodic vacuum arc (FCVA) system as a function of the substrate temperature. The experimental details of this are exactly the same as those described in the original work.<sup>8</sup> Raman and Young’s modulus measurements were performed on  $ta$ -C samples deposited at 90 eV ion energy on (001) Si

substrates taken from the original study. The  $sp^3$  fraction of the films was measured via electron energy loss spectroscopy (EELS). The band gap was measured using an UV-VIS spectrophotometer. The Young’s modulus of the films was measured using laser induced surface acoustic waves (LISAW).<sup>12</sup> The Raman spectra were acquired using the 514 nm line of an Ar ion laser and with a Jobin–Yvon micro-Raman double spectrometer with a spectral resolution of  $\approx 4$ –6  $\text{cm}^{-1}$ . Care was taken to avoid any sample damage.

Figure 1 shows the variation of optical band gap,  $sp^3$  fraction, and resistivity with deposition temperature. It can be seen that the  $sp^3$  fraction remains approximately 80%

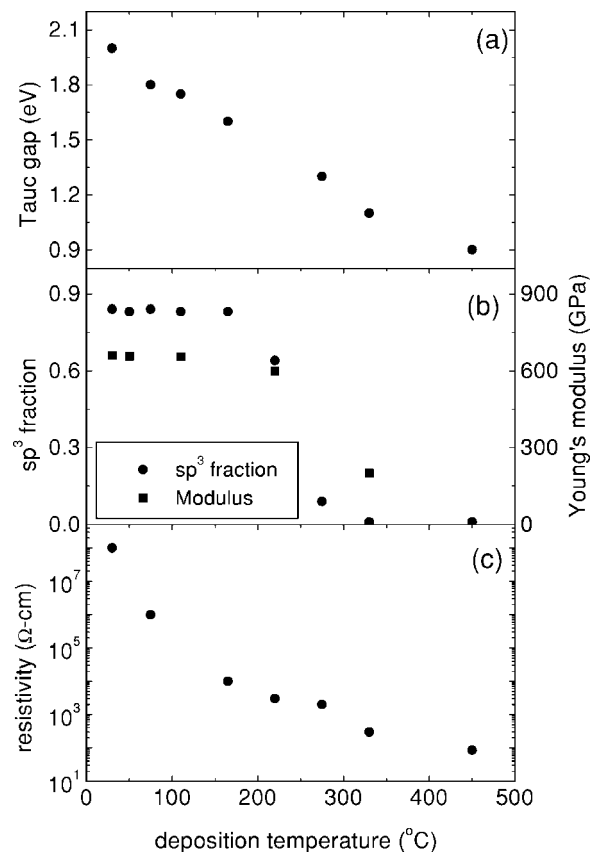


FIG. 1. (a) Optical band gap (b)  $sp^3$  fraction and Young’s modulus and (c) resistivity vs the deposition temperature. The band gap and resistivity fall gradually while the  $sp^3$  fraction and Young’s modulus show a sharp transition.

<sup>a)</sup>Electronic mail: mc209@eng.cam.ac.uk

$\pm 5\%$  for films deposited below room temperature up to  $\approx 200^\circ\text{C}$ , above which there is a sharp transition from 80% to  $\sim 0\%$   $sp^3$  bonding at  $\sim 250^\circ\text{C}$ . Note that the transition temperature of  $\sim 250^\circ\text{C}$  for loss of  $sp^3$  phase during deposition is significantly less than the thermal stability of a  $ta$ -C film deposited at room temperature (RT), and subsequently annealed ( $\sim 1100^\circ\text{C}$ ).<sup>10,13,14</sup> In contrast to the  $sp^3$  fraction, the optical band gap and resistivity are observed to decrease gradually just above room temperature (Fig. 1).

The gradual change in the optical gap and resistivity even when the  $sp^2$  fraction remains constant can be reconciled by understanding of the behavior of the  $sp^2$  sites. Visible Raman spectroscopy using a 514 nm Ar laser allows the direct probe of the  $sp^2$  phase in  $ta$ -C because this photon energy preferentially excites the  $\pi$  states associated with  $sp^2$  sites. The higher sensitivity of Raman at 514 nm to  $\pi$  states is reflected in the higher cross section of graphite than bulk diamond.<sup>15</sup>

The Raman spectra of  $ta$ -C films deposited at various different temperatures are plotted in Fig. 2. The spectra consist of a  $G$  peak at  $\sim 1560\text{ cm}^{-1}$  and a  $D$  peak at about  $1350\text{ cm}^{-1}$ . The  $G$  peak was fitted using a Breit–Wigner–Fano (BWF) function<sup>16</sup> and the  $G$  band position was taken as the maximum of BWF rather than its center.<sup>10</sup> A prominent second order Si substrate peak at  $\sim 960\text{ cm}^{-1}$  occurs in the RT-deposited  $ta$ -C as this film is highly transparent. An additional Lorentzian  $D$  peak is required to describe the Raman spectra of films deposited above  $50^\circ\text{C}$ . The existence of a  $D$  peak indicates the presence of aromatic rings. The  $G$  peak for carbon materials arises from vibrations of all  $sp^2$  sites and in both chain or ring configurations. The intensity of a  $D$  peak however arises only from clusters of  $sp^2$  sites in six fold aromatic rings.<sup>17,18</sup> The  $D$  peak increases with the deposition temperature. The shape of the Raman spectra for the film deposited at  $400^\circ\text{C}$  is indicative of a nanocrystalline graphite. Indeed, small crystallites of graphite are present under transmission electron microscopy (TEM) observations for an  $a$ -C film deposited at  $400^\circ\text{C}$  by FCVA.<sup>8</sup>

Figure 3 shows the ratio  $I(D)/I(G)$  of the  $D$  and  $G$  peaks,  $G$  peak full width half maximum (FWHM) and the  $G$  peak position as a function of the deposition temperature. We see that all values vary gradually with the deposition temperature without any abrupt change at  $250^\circ\text{C}$ , consistent with the optical gap and resistivity, and in contrast to the  $sp^3$  fraction and Young's modulus. Note that  $I(D)/I(G)$  begins to increase above  $50^\circ\text{C}$ , well below the transition temperature.

Considering only those films deposited below the transition temperature of  $250^\circ\text{C}$ , it can be seen that although the  $sp^3$  fraction measured using EELS remains nearly constant, the optical and electrical properties and the Raman characteristics associated with the  $sp^2$  sites gradually decrease. This can be described as follows. For films deposited at RT or below, the material is highly  $sp^3$  bonded with only short olefinic  $sp^2$  chains dispersed within this  $sp^3$  matrix.<sup>19</sup> For these films, the small number of  $sp^2$  sites limits the formation of clusters so that the band gap and resistivity remain high. As the deposition temperature increases above RT, the  $sp^2$  sites begin to diffuse and condense into clusters of increasing size. Aromatic rings form and produce a  $D$  peak in

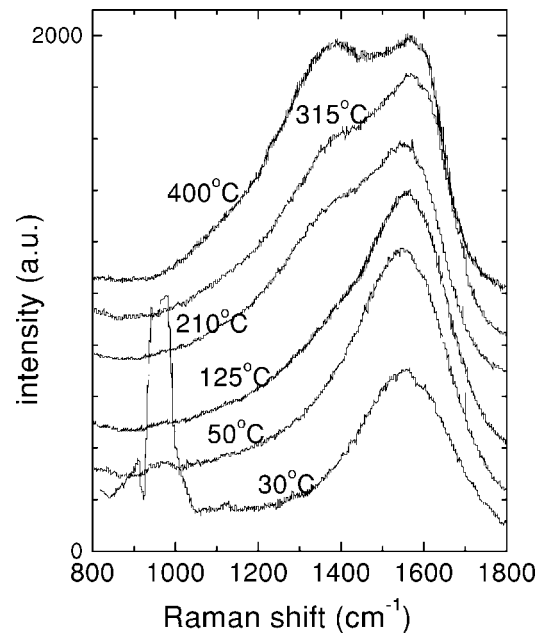


FIG. 2. Raman spectra for  $a$ -C films deposited from 30 to  $400^\circ\text{C}$ .

the Raman spectrum. The appearance of the  $D$  peak well below the transition temperature clearly indicates that the  $sp^2$  sites begin to form aromatic clusters well before a significant decrease in the  $sp^3$  fraction occurs. The  $I(D)/I(G)$  ratio is not a measure of the fraction of the  $sp^2$  phase but of the ordering of the  $sp^2$  phase.

The above results can be put on a quantitative basis using the recently developed model of Ferrari and Robertson<sup>17</sup> of the Raman spectra of disordered carbons. These authors showed how the visible Raman spectra depend primarily on the ordering of  $sp^2$  sites and not on the fraction of  $sp^2$  sites. They showed how the  $I(D)/I(G)$  ratio varies with the  $sp^2$  cluster size. In  $a$ -C, where the disorder is high and cluster size is under 1–2 nm, the  $I(D)/I(G)$  ratio is found to be proportional to the number of aromatic rings  $M$  in the cluster, or  $I(D)/I(G) \propto M$ . It was previously shown that the band gap ( $E_g$ ) of aromatic clusters varies with the cluster size according to  $E_g \propto 1/M^{0.5}$  for undistorted clusters.<sup>6</sup> It was later shown that this relationship overestimates the degree of aromatic ordering of the  $sp^2$  phase in as-deposited diamond-like carbons,<sup>20</sup> but it is valid when a Raman  $D$  peak is prominent, as this indicates the presence of aromatic rings. Therefore it follows that  $I(D)/I(G) \propto E_g^{-2}$ . A plot of the  $I(D)/I(G)$  vs  $E_g^{-2}$  is shown in Fig. 4. The solid line indicates a linear fit and represents the experimental data well. Note that this relationship is followed over the entire temperature range, implying a smooth development of the  $sp^2$  clusters with the deposition temperature, even around the sudden drop in the  $sp^3$  fraction at  $250^\circ\text{C}$ .

The ability of the  $sp^2$  sites to condense into larger clusters while the  $sp^3$  fraction remains fixed indicates that the  $sp^2$  sites act like defects in the  $sp^3$  matrix and can diffuse within it. It also means that the  $sp^2$  sites diffuse at a lower energy than that required to convert  $sp^3$  sites into  $sp^2$  sites. This accounts for the lower annealing temperature of  $sp^2$  rich  $a$ -C than of  $sp^3$  rich  $ta$ -C.<sup>10,21</sup> Another consequence is that above the transition temperature, the newly converted  $sp^2$  sites will also condense into clusters to the same degree

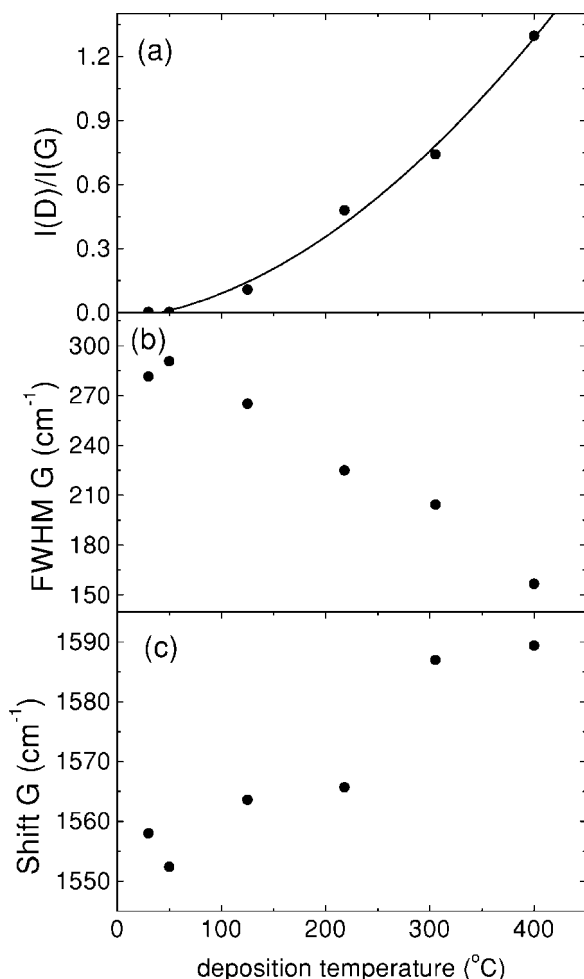


FIG. 3. (a)  $I(D)/I(G)$  ratio, (b) FWHM of the  $G$  peak, and (c) shift in the  $G$  peak position of Raman spectra vs the deposition temperature. Note that all values vary gradually. The solid curve in (a) represents a quadratic fit.

as the already existing  $sp^2$  sites. Thus, the newly formed  $sp^2$  sites cluster in the same way since their diffusion energy is less than the conversion energy.

Figure 1 shows that the resistivity begins to fall before the optical gap.<sup>8</sup> The resistivity is controlled by hopping, so the resistivity can decrease even before the formation of aromatic clusters is evident as a  $D$  peak due to a decrease in the average hopping distance between clusters.<sup>10</sup>

We have also plotted the variation of Young's modulus with deposition temperature in Fig. 1(b). We see that the Young's modulus changes abruptly, like the  $sp^3$  content. Hence, highly  $sp^3$   $ta$ -C film can be viewed structurally as a rigid matrix consisting of  $sp^3$  diamond-like bonds in which short chains of  $sp^2$  sites are embedded. The  $sp^2$  sites can rearrange within the stable rigid  $sp^3$  matrix without strongly influencing the mechanical properties. However, if the  $sp^3$  matrix collapses or the amount of  $sp^3$  sites is reduced, then the mechanical properties such as hardness and Young's modulus will also decrease. Figure 1(b) shows that the variation of the Young's modulus correlates well with the average  $sp^3$  fraction, in agreement with the conclusion that the mechanical properties of  $ta$ -C are primarily dependent on the mean coordination.<sup>7</sup> Other reports also found that the hardness and Young's modulus of  $ta$ -C films measured using nanoindentation and LISAW do not change as long as the  $sp^3$  fraction is maintained.<sup>12-14</sup>

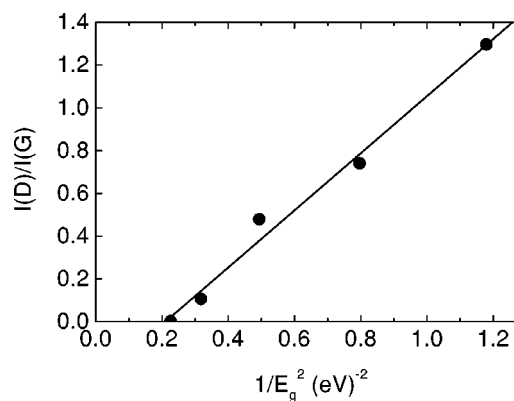


FIG. 4. Raman  $I(D)/I(G)$  ratio vs  $E_g^{-2}$ . The solid curve represents a linear fit.

In conclusion, we have shown that the Young's modulus of  $ta$ -C is primarily dependent on the  $sp^3$  phase while the optical and electrical properties are strongly influenced by the quality of the  $sp^2$  phase. We have monitored the  $sp^2$  phase using visible Raman spectroscopy. The Raman characteristics such as the  $I(D)/I(G)$ ,  $G$  peak position and FWHM were found to change gradually with the deposition temperature, consistent with the optical and electrical properties of the films. In addition, the  $I(D)/I(G)$  was found to vary quadratically with the inverse of the band gap. These results show how moderate annealing can be used to modify the  $sp^2$  nanostructure almost independently of the  $sp^3$  phase and can reconcile different electronic and optical properties reported in the literature for  $ta$ -C with the same  $sp^3$  content.

M.C. acknowledges the financial and collaborative support from Multi-Arc Inc. A.C.F. acknowledges an EU Marie Curie fellowship.

- <sup>1</sup>D. R. McKenzie, D. Muller, and B. A. Pailthorpe, Phys. Rev. Lett. **67**, 773 (1991).
- <sup>2</sup>J. Robertson, Surf. Coat. Technol. **50**, 185 (1992).
- <sup>3</sup>P. J. Fallon, V. S. Veerasamy, C. A. Davis, J. Robertson, G. A. J. Amaratunga, and W. I. Milne, Phys. Rev. B **48**, 4777 (1993).
- <sup>4</sup>Y. Lifshitz, Diamond Relat. Mater. **5**, 388 (1996).
- <sup>5</sup>I. Robertson, Diamond Relat. Mater. **3**, 361 (1994).
- <sup>6</sup>J. Robertson and E. P. O'Reilly, Phys. Rev. B **35**, 2946 (1987).
- <sup>7</sup>J. Robertson, Phys. Rev. Lett. **68**, 220 (1992).
- <sup>8</sup>M. Chhowalla, J. Robertson, C. W. Chen, S. R. P. Silva, C. A. Davis, G. A. J. Amaratunga, and W. I. Milne, J. Appl. Phys. **81**, 139 (1997).
- <sup>9</sup>S. Sattel, J. Robertson, and H. Ehrhardt, J. Appl. Phys. **82**, 4566 (1997).
- <sup>10</sup>A. C. Ferrari, B. Kleinsorge, N. A. Morrison, A. Hart, V. Stolojan, and J. Robertson, J. Appl. Phys. **85**, 7191 (1999).
- <sup>11</sup>J. Robertson, Phys. Rev. B **53**, 16302 (1996).
- <sup>12</sup>D. Schneider, B. Schultrich, H. I. Scheibe, H. Ziegele, and M. Griepentrog, Thin Solid Films **332**, 157 (1998).
- <sup>13</sup>T. A. Freidmann, J. P. Sullivan, J. A. Knapp, D. R. Tallant, D. M. Follstaedt, D. L. Medlin, and P. B. Mirkarimi, Appl. Phys. Lett. **71**, 3820 (1997).
- <sup>14</sup>S. Anders, J. W. Ager, G. M. Pharr, T. Y. Tsui, and I. G. Brown, Thin Solid Films **308**, 186 (1997).
- <sup>15</sup>N. Wada, P. J. Gaczi, and S. A. Solin, J. Non-Cryst. Solids **35**, 543 (1980).
- <sup>16</sup>S. Praver, K. W. Nugent, Y. Lifshitz, G. D. Lempert, E. Grossman, R. Kalish, and Y. Avigal, Diamond Relat. Mater. **5**, 433 (1996).
- <sup>17</sup>A. C. Ferrari and J. Robertson, Phys. Rev. B (to be published).
- <sup>18</sup>C. Mapelli, C. Castiglioni, G. Zerbi, and K. Mullen, Phys. Rev. B **60**, 12710 (1999).
- <sup>19</sup>D. A. Drabold, P. A. Fedders, and M. P. Grumbach, Phys. Rev. B **54**, 5480 (1996).
- <sup>20</sup>J. Robertson, Diamond Relat. Mater. **4**, 297 (1995).
- <sup>21</sup>S. Bhargava, H. D. Bist, A. V. Nalikar, S. B. Samanta, J. Narayan, and B. Tripathi, J. Appl. Phys. **79**, 1917 (1996).